Research Article Vol. 28, No. 4 / 17 February 2020 / Optics Express 4550
Optics EXPRESS

Widely-tunable mid-infrared ring cavity pump-enhanced OPO and application in photo-thermal interferometric trace ethane detection

JACK W. THOMAS,[1,2,*] ADAM POLAK,[1] GERALD M. BONNER,[1] DAVID LOGIE,[3] MALCOLM H. DUNN,[2] JONATHAN C. F. MATTHEWS,[4] AND DAVID J. M. STOTHARD[1]

[1] *Fraunhofer Centre of Applied Photonics, Technology and Innovation Centre, 99 George Street, Glasgow, G1 1RD, UK*
[2] *School of Physics and Astronomy, University of St Andrews, North Haugh, St Andrews, Fife KY16 9SS, UK*
[3] *Cascade Technologies, Glendevon House, Castle Business Park, Stirling, FK9 4TZ, UK*
[4] *Quantum Engineering Technology Labs, H. H. Wills Physics Laboratory and Department of Electronic and Electronic Engineering, University of Bristol, Tyndall Avenue, Bristol, BS8 1FD, UK*
[*] *jt94@st-andrews.ac.uk*

Abstract: The development of a broadly and accurately tunable single-frequency mid-infrared laser source and its application to a sensitive laser absorption detection method are described. Photo-thermal interferometric spectroscopy is employed as a phase-sensitive method to detect the minute refractive index change caused by the heating of a gas under laser radiation. A separate probe beam allows for the spectrally-interesting mid-infrared region to be examined whilst utilizing low cost, high detectivity photodetectors in the visible/near-infrared region. We also describe the implementation of a Sagnac interferometer to minimize the effects of environmental perturbation and provide inherent passive stability. A continuous-wave ring-cavity pump-enhanced OPO has been developed to provide excitation light from 3–4 μm at 140 mW with the ability to mode-hop tune continuously over 90 cm^{-1} in 0.07 cm^{-1} steps. Complementary use of both detection apparatus and excitation source has allowed for presence of ethane to be detected down to 200 parts per billion.

1. Introduction

The phenomenon of optical absorption allows for identification of substances through measurement of their characteristic spectral absorption features. This principle can most simply be applied using a single-pass geometry from the output of a tunable light source to provide spectral information by observing the spectral regions where the transmitted light is distinguishably attenuated. Detection of trace concentrations of molecules is difficult using this simplistic approach as the reduced optical-molecular interaction results in weak absorption, which then requires complex cooled detectors in the mid- to deep-infrared spectral region where many molecules of interest exhibit their strongest and most characteristic features [1]. Enhancements of this technique increase optical molecular interaction by utilizing multi-pass cells [2] and cavity-enhancement [3] to achieve significant improvements in sensitivity, though these devices are still reliant on direct detection of the infrared beam and hence cooled mid- /deep-infrared detectors.

Alternately, the effects of the absorption can be *indirectly* observed by means of monitoring the conditions of the gas. The heat absorbed can be exhibited commonly in either a pressure

#385603 https://doi.org/10.1364/OE.385603
Journal © 2020 Received 12 Dec 2019; revised 13 Jan 2020; accepted 18 Jan 2020; published 3 Feb 2020

Optics EXPRESS

wave, leading to photo-acoustic effects [4] or by an increase of temperature—this work focuses on the latter. This is typically of a small magnitude creating considerable difficulty to be detected by electrical means of a thermocouple so optical means are required. These approaches have included the use of an infrared camera to detect the thermally-induced infrared emission from excited surfaces [5], and monitoring the thermally-induced beam deflection of either a monitored probe beam [6] or intra-cavity of a monitored probe laser [7]. The method we describe here builds on the use of a collinear probe beam of an interferometer where the phase change detected is inductive of the increase in gas temperature of photo-thermal heating of the tunable excitation beam [8]. This has been applied to great effect demonstrating sensitivities on the order of 10 parts-per-billion volume concentration whilst detecting gases such as SF_6 using deep-infrared excitation sources [9,10]. Crucially, this technique allowed the absorption-induced phase-changes to be detected using the visible probe light from a He-Ne laser and uncooled silicon photodetectors which were low-noise, low cost and exhibited high detectivity (D*), whilst simultaneously exploiting absorption features in the deep infrared using a suitable excitation laser (a tunable CO_2 laser in the case of Ref. [9]).

Our work includes two important refinements on this previous activity, relating to both the source and the interferometric detection arrangement. Firstly, we avoid sensitivities to environmental mechanical perturbation exhibited by the Mach-Zehnder interferometer by utilizing a passively stable, dual beam Sagnac interferometer removing any requirement for optical path length stabilizing equipment. This device exhibits counter propagating interfering beams that share a near common path such that any ambient noise manifests itself in the common mode of each beam and is therefore suppressed. A commercial single-frequency 1.064 μm laser is used as the internal probe beam to remove potential beating issues. Ethane gas is detected in this investigation due to the distinguishable mid-infrared absorption features and the similar relative mass of the molecule with air allowing for mixing consistency. Instead of the formerly applied pulsed CO_2 laser, this work uses continuous-wave excitation light in the 3 –4 μm spectral region for greater spectral resolution which is generated by an Optical Parametric Oscillator (OPO) [11]in lieu of traditional laser sources in this spectral region. Numerous investigations have utilized OPOs to detect hydrocarbons at trace concentrations [12–16] with a range of detection techniques. This work employs a pump-enhanced OPO [17] in order to efficiently down-convert 1.064 μm to the required mid-infrared wavelengths with the non-linear medium and phase-matching provided by Periodically Poled Lithium Niobate (PPLN) [18]. Ring-cavity designs have shown potential for high-resolution mode-hop tuning [19] by using an adjustable intra-cavity etalon to provide frequency-distinguishing properties, and dual-cavity standing-wave systems [20] can provide for frequency-selective elements with less complex coatings and even open the possibility of mode-hop-free tuning due to the removal of cavity length constraints. The pump-enhanced OPO established in this work benefits from both the ring-cavity and dual-cavity approaches by using a split-ring design with an intra-cavity etalon in the signal cavity. The spectral resolution of this device is combined with the sensitivity of photo-thermal detection in the split-Sagnac design for spectroscopy.

2. Photo-thermal modelling

We first present a simple analysis to indicate the sensitivity of the instrument for a given target-gas concentration, excitation power and interaction length in order to show the efficacy of our approach. The radiation absorbed (P_A) by the constituent gas at corresponding transition frequencies is transferred from optical power to the temperature of the gas. This can be described by considering the incident power (P_I), the interaction path length (z), and the absorption coefficient of the gas (α_ν) determined by the ethane concentration and the excitation beam optical frequency (ν) in Eq. (1).

$$P_A = P_I[1 - e^{-\alpha_\nu z}] \tag{1}$$

Optics EXPRESS

The spatial heat distribution (Q(r,z)) can be derived by applying the absorbed laser power as a function of length with the beam radius (w(z)) relation defined by knowing the position (z_0), the wavelength (λ) and size of the beam waist (w_0) to provide the radial (r) distribution of the energy. A simple integration bound by the condition in Eq. (1) leads to the condition determining the heating effect of the excitation light in Eq. (2) with w(z) shown in Eq. (3).

$$Q(r, z) = P_I \frac{2\alpha_\nu}{\pi w^2(z)} e^{-\frac{2r^2}{w^2(z)} - \alpha_\nu z} \tag{2}$$

$$w^2(z) = w_0^2 \left(1 + \left[\frac{(z - z_0)\lambda}{\pi w_0^2}\right]\right) \tag{3}$$

The heat deposition is converted into a spatial and temporal temperature increment by consideration of environmental heat transfer coefficients using modelling software COMSOL'. Our simulations considered a modulated excitation beam at 200 Hz, varying gas cell lengths between 2 and 20 cm and examining ethane at concentrations between 10^{-1} - 10^5 parts per million. We simulated excitation light tuned to the 2987 cm^{-1} absorption line of C_2H_6, which exhibited an absorption coefficient of 0.56 cm^{-1} at 10^5 parts per million and scaled linearly with concentration and an excitation power of 50 mW. Figure 1 displays the typical dynamics and spatial qualities of the photo-thermal heating. The time evolution shows that at a modulation frequency of 200 Hz, the thermal time constant of the gas-air mixture is too long to rise to a

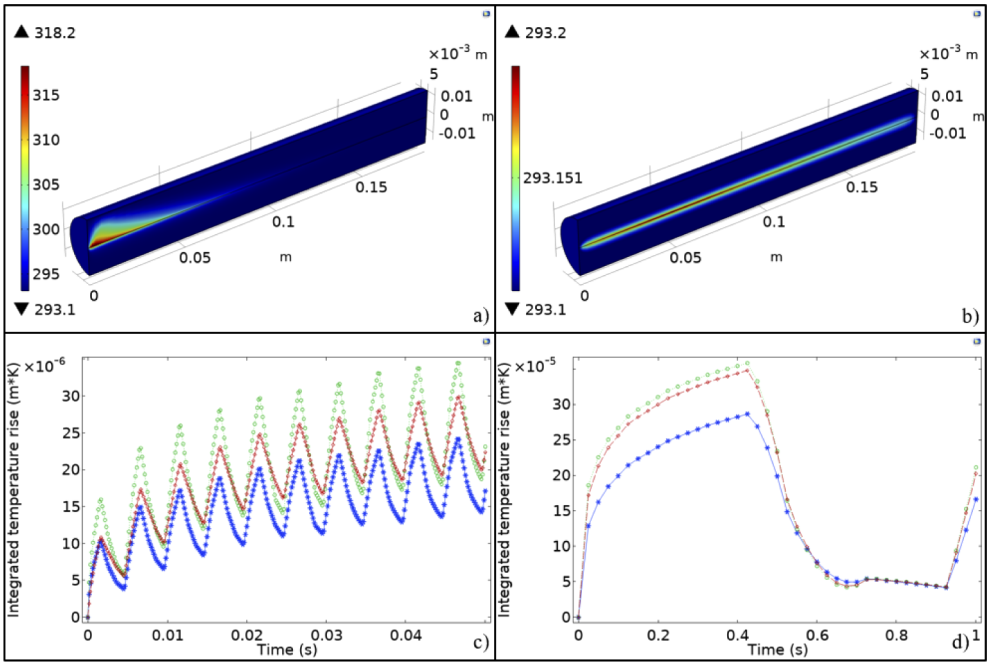

Fig. 1. Color maps of temperature of gas cell under laser absorption with a beam waist of 50 µm at a high concentration of gas [10^4 ppm] a) and low concentrations of gas [1 ppm] b). Temporal responses with different beam waists at a low concentration of gas [10 ppb] showing the integrated temperature rise [temperature change integrated over length] with 200 Hz modulation c) and 1 Hz modulation d) [red, green, and blue traces correspond to excitation beam waist radii of 0.5, 0.1 and 0.05 mm respectively]. Model is initiated with and has cylinder boundaries at 25 °C with a cylinder length of 188 mm and diameter of 25 mm.

Optics EXPRESS

steady state, whereas a study over a longer duration shows approximately 0.15 s to be a sufficient period to maximize the heating. However, this corresponds to a modulation frequency of 2-3 Hz, which is undesirable due to the magnitude of the 1/f noise in this region.

Temperature changes throughout a path length can be translated to optical path length changes by consideration of the dependence of air's refractive index on temperature, calculated in other works [21]. A phase shift can be calculated by taking the ratio of this effective length change with the wavelength of the probe light; in this case 1.064 µm. From this, the expected modulating signal from a correctly aligned interferometer, operating from halfway up a fringe, can be predicted as shown in Fig. 2. This therefore gives the expected sensitivity per volume concentration and shows routes for optimization. The photo-thermal effect increases linearly with concentration showing a predicted signal of 50 µV at 100 parts per billion volume concentration [marked 'I' in Fig. 2(a)], with saturation shown at higher concentrations of ~ 10^4 parts per million volume concentration where the energy of the incident beam is fully absorbed within the cell (marked 'II'). A negligible differential response is present (marked 'III') above this because the energy of the excitation beam is absorbed before the focal point, giving heat deposition over a wider area and therefore reducing the temperature change per unit length. Considerations with regard to optimal focusing and interaction length show that as expected a longer interaction length is desirable, and optimum focusing is strongly dependent on the interaction length where a greater temperature change will be achieved at the focus with a smaller waist but a greater distribution of energy will occur with greater collimation in longer gas cells.

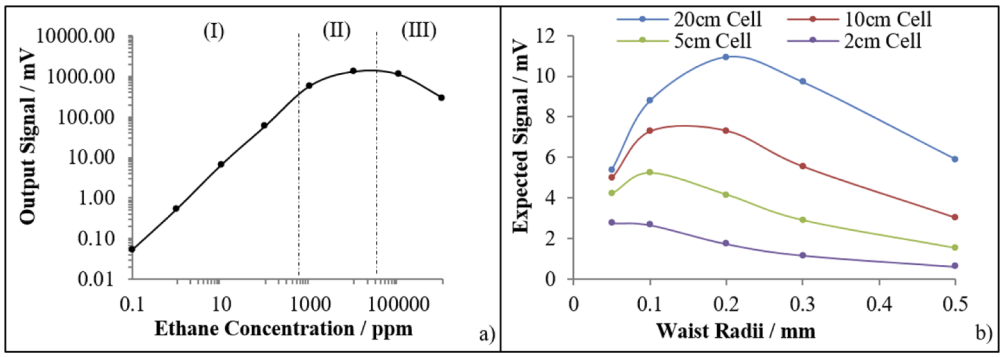

Fig. 2. Model results showing the predicted signal given an 8 V peak-to-peak fringe visibility showing the sensitivity of the technique in terms of ethane concentration when focused to a 50 µm waist in a 20 cm cell a) and depicting the optimum focusing conditions of the excitation beam provides different gas cell lengths with a concentration of 10 ppm ethane b).

3. Split-ring pump-enhanced OPO excitation source

The tunable excitation source in this experiment is a pump-enhanced continuous-wave OPO based upon 5% MgO:PPLN. The crystal has dimensions of $28 \times 15 \times 1$ mm and exhibits fan-out poling for broad phase-match tuning via translation, varying the poling-period through the width from ~ 27–32 µm. The device is pumped by 1.35 W of single-frequency 1.064 µm radiation provided by a Coherent Mephisto laser. Under this pump wavelength, the quasi-phase-matching allows for a tuning-range between 1.4–1.7 µm in the resonant signal and 2.8–4.5 µm in the non-resonant idler. The crystal has been coated accordingly for anti-reflective surfaces at 1.064 µm, 1.44–1.68 µm, and 2.9–4.1 µm and is mounted in an oven and maintained at a constant temperature of 35 °C by means of a DN515-1528 proportional heater. The cavity configuration is shown schematically in Fig. 3 employing a travelling-wave resonator, with the mode of the parent pump Mephisto laser carefully matched into the resonant ring cavity using a single 100 mm focal length lens, and

Optics EXPRESS

separate ring for signal resonance distinguished by dichroic beam splitters. This allows the signal cavity to be altered for tuning purposes without affecting the resonant pump. The pump cavity operating at 1.064 µm is formed by mirror M1 (90% reflective) and mirrors M2, M7, and M8, all high-reflectors with the latter piezo-actuator mounted for Pound-Drever-Hall locking giving a power enhancement of 10. The signal cavity operating between 1.42–1.63 µm shares mirrors M1 and M2, high-reflectors, and mirrors M3, M4, M5, and M6, high reflectors and dual-band highly transmitting at 1.064 µm. Mirror M2 is highly transmitting at 3–4 µm and made with CaF_2 to allow the idler field to exit the cavity after a single pass through the PPLN crystal. Precision control of the resonant signal wave is provided by a piezo-actuated intra-cavity air-space etalon E (manufactured by Light Machinery [22]) with a free-spectral-range of 330 GHz (11 cm^{-1}) and coated for 40% reflectivity at 1.4-1.65 µm. Two tuning schemes are designed into this system; the PPLN crystal can be translated axially through the cavity to utilize different poling periods for course tuning over 3-4 µm, and then the OPO can be finely tuned by hopping adjacent cavity modes (~0.02 cm^{-1}) over its phase matching bandwidth (ultimately, this is limited by the 11 cm^{-1} FSR of the etalon). Whilst smooth and continuous, mode-hop free tuning would be desirable, our approach of hopping on near-adjacent cavity modes was simple to implement and exhibited a tuning resolution more than adequate to resolve pressure-broadened spectral features down to ~2kPa.

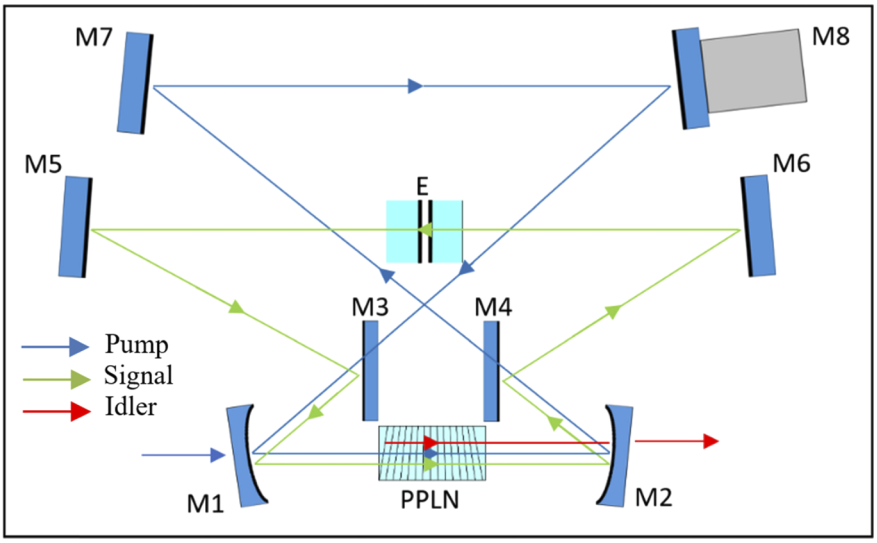

Fig. 3. Schematic of split-ring pump-enhanced OPO based upon PPLN depicting the two joined cavities resonating the pump frequency (blue) and the signal frequency (green) with the idler non-resonant (red). The pump cavity consists of an input coupler (M1) of ROC 100 mm, a double high reflector (M2) of ROC 100 mm, two dichroic beam splitters (M3 & M4), and two plane pump high reflectors (M7 & M8 w/ piezo). The signal cavity is completed with plane signal high reflectors (M5 & M6) and a signal coated air-spaced etalon (E).

The operational performance of the OPO is displayed graphically in Fig. 4 showing an external pump power threshold of ~ 200 mW (i.e. ~ 2 W single-direction circulating field within the enhancement cavity) when generating idler light at 3.35 µm with a maximum recorded idler power of 130 mW whilst pumped by 850 mW of pump light at 48% conversion efficiency. Broad tuning of the idler via translation of the fan-out PPLN through the cavity can access mid-infrared wavelengths between 3–4 µm whilst providing > 80 mW for much of this range.

Optics EXPRESS

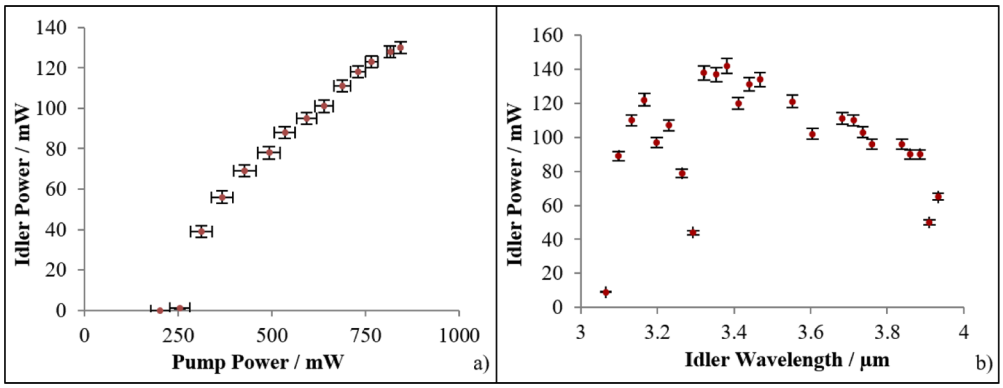

Fig. 4. Operational performance of the split-ring PE-OPO showing the conversion efficiency a) and the broad tuning range via translation of the PPLN through the cavity b).

Fine-tuning is provided by voltage adjustment across the air-spaced etalon piezo-actuator which was controlled via Labview using the analogue output of an MCCDAQ device in combination with a 10x voltage amplifier. A Highfinesse WS7 wavemeter was used to detect the output signal frequency, from which the idler frequency is calculated. The results of tuning the etalon with voltage are displayed in Fig. 5 showing that the entire free-spectral-range of 11 cm^{-1} of the etalon is accessible. The power variation as the signal and idler is tuned about the center of the PPLN phase matching bandwidth is clearly visible (red trace) and this was kept above 85% of the power at line center for the 11 cm^{-1} tuning range. Tuning resolution was limited to steps of 0.07 cm^{-1} (~2 GHz) equating to mode-hop tuning of 4 longitudinal modes of the cavity. This optical frequency transition corresponds to the free-spectral-range of the PPLN crystal (~ 0.077 cm^{-1}) where the finite facet reflections at the signal wave were responsible for causing weak and unwanted selectivity; thus limiting the resolution available. Superior anti-reflection coatings (currently 0.5%) or wedged surfaces would reduce this issue.

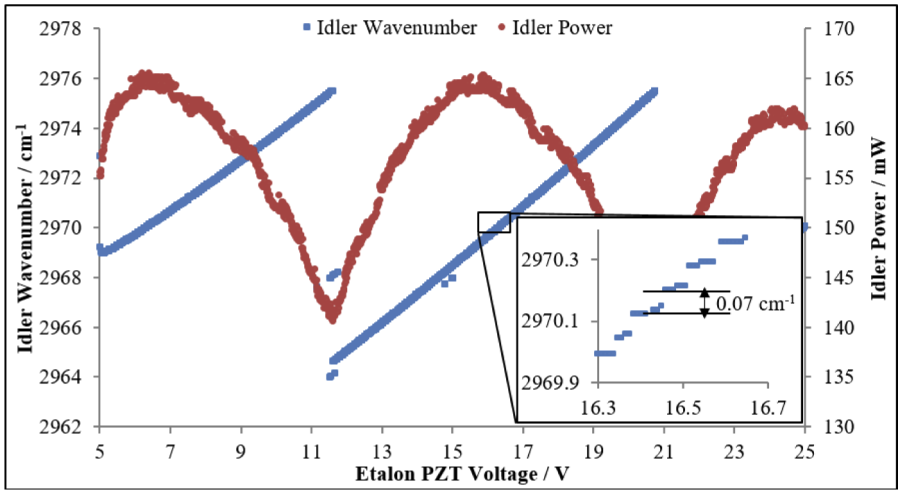

Fig. 5. Fine-tuning range of split-ring PE-OPO by voltage applied to the piezo-actuator in the air-spaced etalon.

Synchronizing the fine-tuning of the etalon with the course-tuning of the crystal translation enables yet larger tuning ranges whilst maintaining the spectral resolution. This is achieved by

Optics EXPRESS

voltage controlling the tuning of the PPLN position by mounting it on a motorized stage (Zaber X-LSM025A) and synchronously tuning the voltage applied to the etalon. A simple step-by-step addition algorithm with different step weightings is used to tune each element. Figure 6 shows that this enabled a significant improvement of > 8x the tuning range to 90 cm^{-1} (~2.5 THz) maintaining high spectral resolution with a step size of 0.07 cm^{-1}. This was limited by the simplistic step-algorithm which did not account for the frequency/voltage non-linearity in each device.

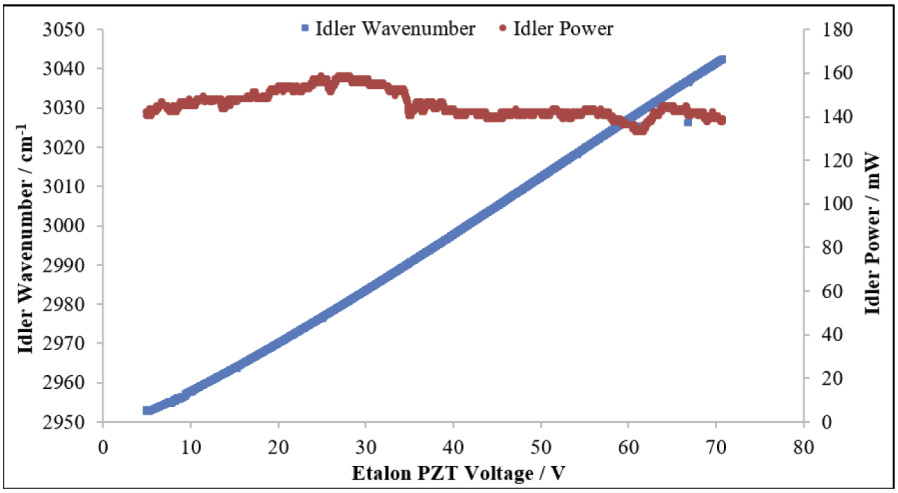

Fig. 6. Extended fine-tuning range of split-ring PE-OPO enabled by synchronous tuning etalon and PPLN translation.

4. Photo-thermal spectroscopy

The interferometer geometry used to detect the photo-thermal heating is a split-Sagnac arrangement shown in Fig. 7. Our earlier work [23,24] utilized a Mach-Zehnder interferometer, but its sensitivity to environmental noise required sensitive stabilization electronics. The inherent stability and insensitivity to noise exhibited by the Sagnac geometry required no locking electronics to retain a mid-point interference fringe position. The probe beam is 10 mW of the 1064 nm of the Mephisto laser used to pump the OPO where the single-frequency nature of the light reduces any noise due to beating effects. A BPX65 silicon photodiode detects the output of the interferometer and through a trans-impedance amplifier provides an 8-volt peak-to-peak interference fringe visibility. In order to align the device at a mid-fringe position for maximum sensitivity, a glass slide is placed such that it is only in the path of one of the two propagating probe beams and tilted to correct the phase. Two silica-based long-pass dichroic mirrors are placed around the gas cell to pass the excitation beam at 80% transmissivity. The gas cell of 20 cm length has windows of uncoated calcium fluoride to due to negligible absorption in the mid-infrared region. The excitation beam is focused by a 100 mm calcium fluoride lens to provide a 50 μm waist within the cell and amplitude modulation a frequency of 240 Hz is provided by a chopper. A lock-in amplifier is used to isolate and demodulate the photodetector output signal to establish the photo-thermal signal, which is then input into the Labview acquisition software via the MCCDAQ.

In order to align and optimize the system, the modulation frequency of the excitation beam was initially applied at low frequencies (2-5 Hz) and tuned to the 2897 cm^{-1} ethane absorption peak with a high (28%) concentration of the gas present exhibiting the fringe modulation shown in Fig. 8. This demonstrated similar heating dynamics to the COMSOL modelling with optimal

Optics EXPRESS

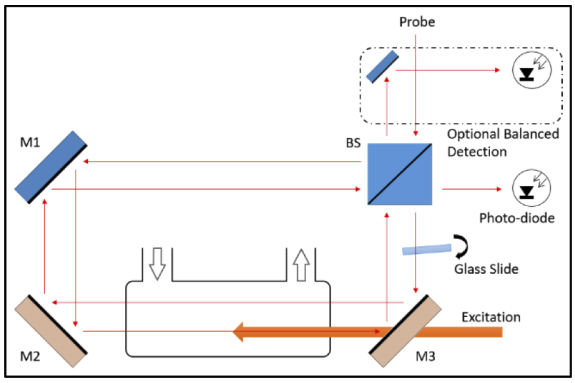

Fig. 7. Schematic of the split-Sagnac interferometer used to detect the photo-thermal effect of laser absorption displaying a 50:50 beam splitter (BS), a folding mirror (M1), two dichroic mirrors (M2 & M3), with an internal probe passing through the gas cell with a collinear excitation beam and the resultant interference detected by a silicon photodiode.

heating occurring on a long (>100 ms) time base at low frequencies, with a reduction in the measured effect due to uncharacterized optical losses and imperfect beam alignment both for the excitation beam and the interferometer. This slow modulation is prone to interference due to the high background noise at low frequencies. Measurements were taken at modulation of 200-240 Hz as the noise reduction is > 40 dB offsets the signal attenuation of < 20 dB. At these higher rates there is a more favorable signal-to-noise ratio and also provides a practical benefit in reducing the time required per measurement (500 ms to 5 ms).

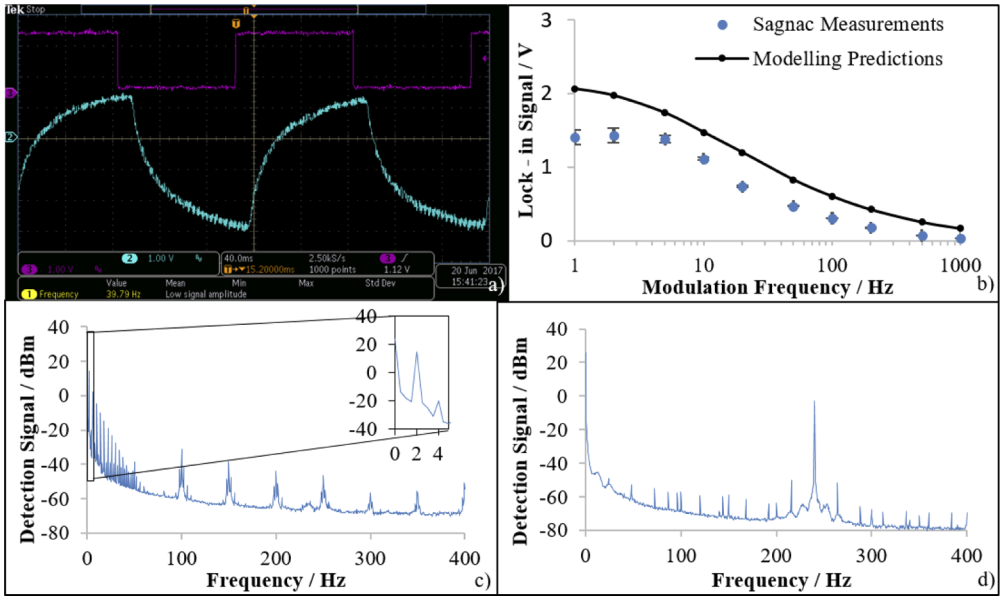

Fig. 8. The dynamic response of the photo-thermal effect (blue) with 5 Hz modulation (purple) of the excitation beam generating a modulation in the interferometer output a) with comparison to modelling predictions at varying modulation frequency b) and frequency representation of signal detected on photodiode at 2 Hz modulation c) and 240 Hz modulation d).

Optics EXPRESS

The OPO source tunes through a range of 2970 - 3010 cm^{-1} whilst logging the acquired photo-thermal signal. The gas samples were prepared using an approximate dilution method by extracting either 10^1 or 10^4 parts per million ethane concentration samples and reducing by mixing with air (where water vapor is present). The resultant spectra shown in Fig. 9 sampled 2 parts per million of ethane, where these absorption features are present alongside those of the water vapor (28% relative humidity) present in the diluting gas. All results are shown alongside the theoretical HiTran2012 spectra obtained for 25 °C and 1 atmosphere. This demonstrates the ability to detect absorption features with a spectral linewidth of 0.15 cm^{-1} and clearly distinguish features separated by 0.9 cm^{-1}.

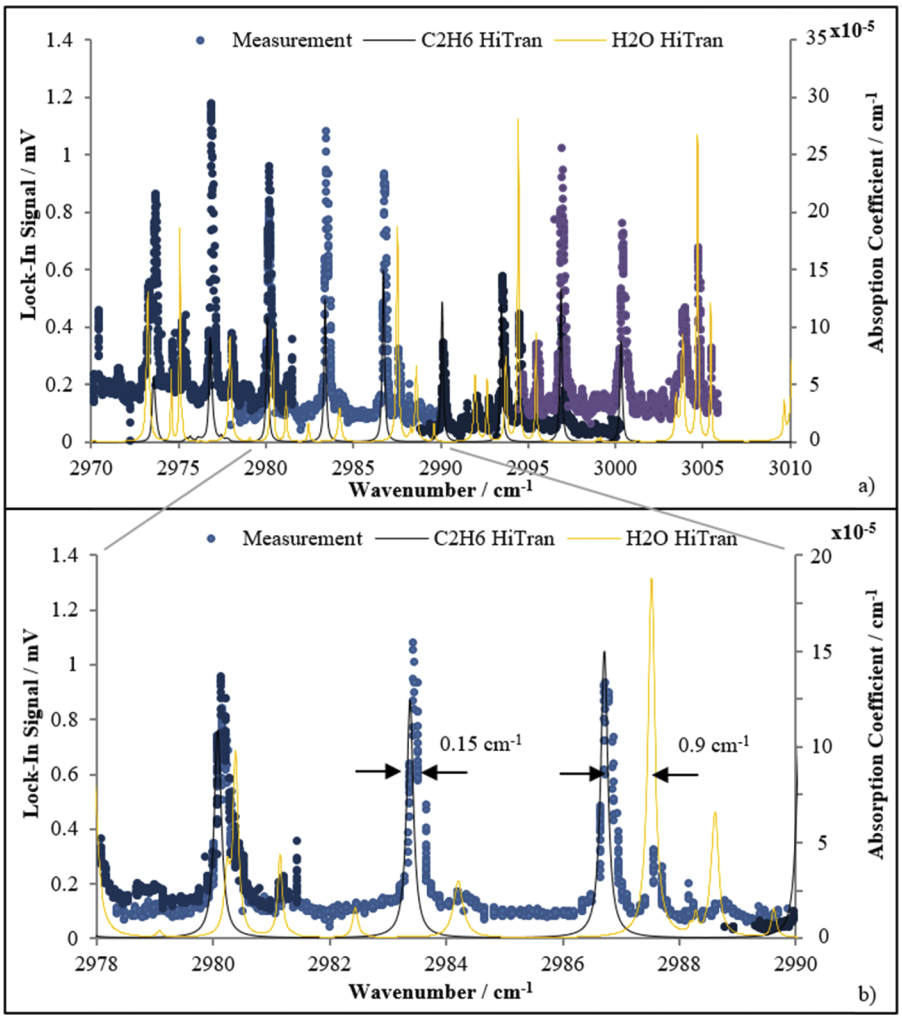

Fig. 9. Spectra of gas sample containing 2 ppm ethane diluted with room air displaying photo-thermal measurements [different colored points indicate a separate measurement run] alongside theoretical HiTran2012 absorption spectra. Displayed across the full 40 cm^{-1} tuning range a) and zoomed to a 12 cm^{-1} range b) to highlight features.

Sensitivity down to 200 parts per billion has been demonstrated by operating the OPO to the peak absorption of ethane (2987 cm^{-1}) and recording the lock-in amplifier signal at reducing concentrations as displayed in Fig. 10. This is limited by the system noise floor at approximately

Optics EXPRESS

0.1 mV. These results followed those expected from the theoretical modelling, with a discontinuity at the sensitivity limitation caused by positive interference by the noise floor. A spectrum taken at the 200 parts per billion in Fig. 11 confirms detection limitation with visible ethane peaks at an approximate signal to noise ratio of 2:1.

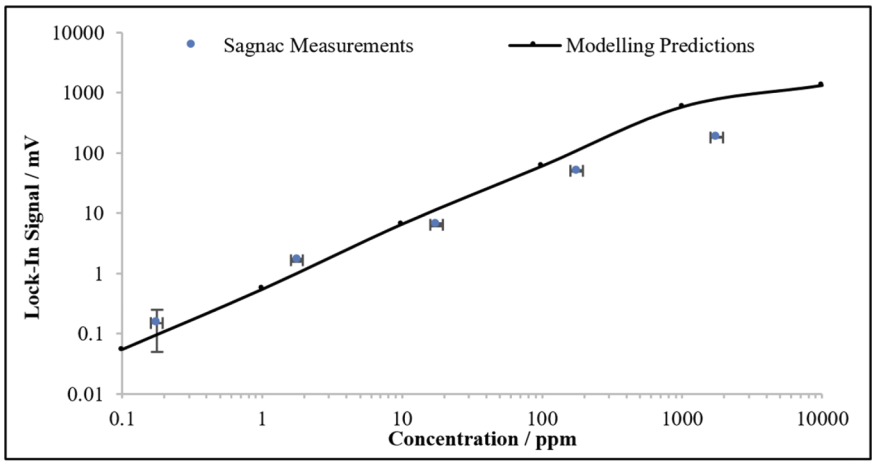

Fig. 10. Sensitivity of Sagnac photo-thermal interferometer when tuned to 2987 cm^{-1} ethane absorption line shown alongside modelled predictions.

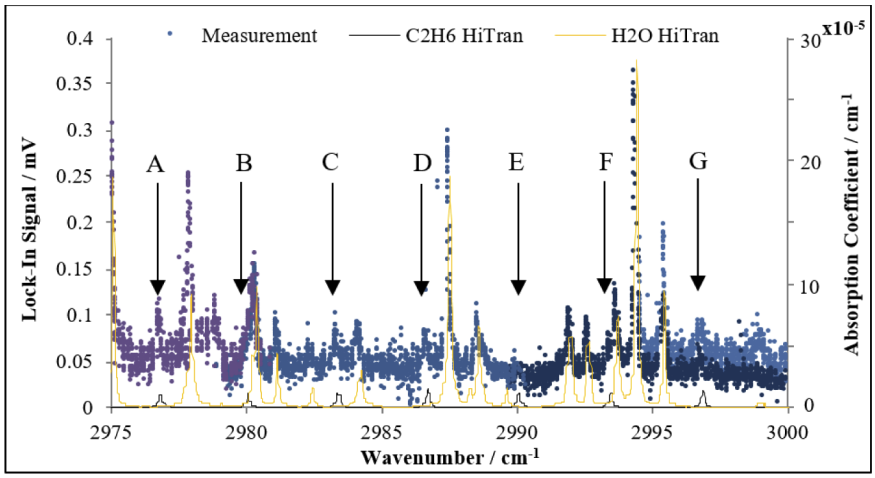

Fig. 11. Spectra of gas sample containing 200 ppb ethane diluted with room air displaying photo-thermal measurements [different colored points indicate a separate measurement run] alongside theoretical HiTran2012 absorption spectra. Arrows display spectral locations of ethane absorption with B & F obscured by water absorption proximity and E obscured by being at transition of OPO tuning.

The limitation of the technique of 200 parts per billion of ethane, corresponding to an absorption coefficient of 10^{-5} cm^{-1}, is due to the noise of the detection apparatus and the laser noise. For more sensitive testing a balanced detector was employed to give a differential measurement utilizing both interferometer output beams. This bespoke detector, based upon an established design [25] utilized two InGaAs photo-diodes with a differential gain of 10^6 optimized for low-noise at low frequencies and is 20x more sensitive than the photodiode and trans-impedance

Optics EXPRESS

amplifier circuit giving an equivalent interferometer fringe visibility of 160 V. Ethane detection at 20 parts per billion is not conclusive with this detector due to the dominance of the water vapor features as shown from the spectra obtained in Fig. 12. However, water vapor features are distinguishable indicating an increased sensitivity to an absorption coefficient of 10^{-6} cm^{-1} which corresponds to a change in optical path length of 0.32 pm, a refractive index change of 1.7×10^{-12}, and an average temperature change of 1.9 μK.

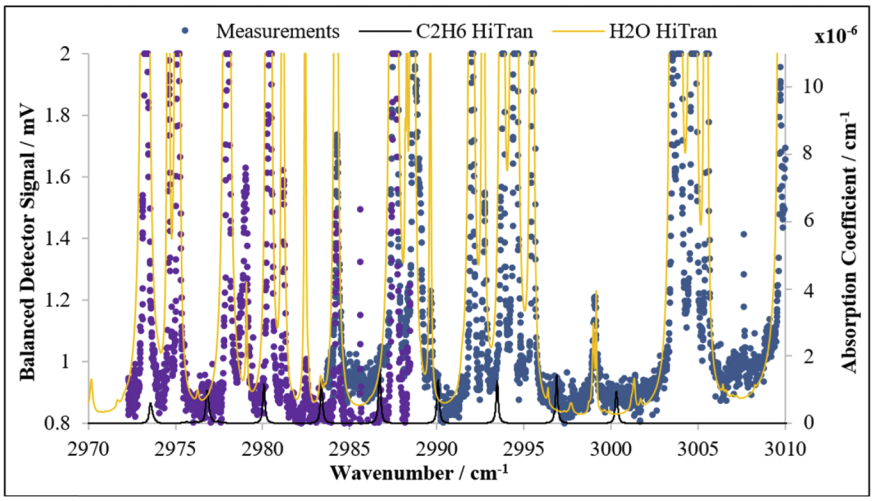

Fig. 12. Spectra of gas sample obtained using homodyne detector to detect 20 ppb ethane diluted in room air [different colored points indicate separate measurement run].

The 0.8-0.9 V offset in the spectra is due to optical heating of the input coupling mirror of the interferometer causing thermal expansion across the entire tunable spectra. This input mirror is made of fused silica and absorbs ~ 10% of the transmitted light. If we consider the thermal expansion coefficient of silica glass ($\sim 0.65 \times 10^{-6}$ K^{-1}) and apply to the theoretical model, this is predicted to be 1.2 V in close agreement with to practical observations. Potential improvements to sensitivity include using calcium fluoride dichroic mirrors to reduce the thermal expansion distortion in the interferometer, reducing the gas pressure at which measurements were taken for a reduction of pressure broadening of absorption peaks, and developing a method of background subtraction to remove water distortion.

5. Conclusion

The photo-thermal effect of laser absorption to detect ethane has been studied in this work. Modelling has confirmed optimal parameters for a maximized phase-change upon photo-thermal heating. A widely tunable pump-enhanced OPO has been constructed which is able to broadly tune between 3 and 4 μm, and exhibits the ability to have automated fine-tuning in 0.07 cm^{-1} steps across a wide range of 90 cm^{-1}. This work specifically has built on previous demonstrations by utilizing an inherently stable interferometer avoiding locking complexities. Uses of a split-Sagnac interferometer to detect the photo-thermal effect has demonstrated detection of ethane to levels of 200 parts per billion which corresponds to an absorption coefficient of 10^{-5} cm^{-1} and resolved water absorption peaks corresponding to 10^{-6} cm^{-1}.

Funding

Innovate UK (133076); Engineering and Physical Sciences Research Council (EP//L01596X/1, EP/M01326X/1, EP/M024385/1); European Research Council (ERC-2018-STG 803665).

Optics EXPRESS

Acknowledgments

JWT acknowledges support from the Centre for Doctoral Training in Applied Photonics. JCFM acknowledges support from the UK Quantum Technology Hub in Quantum Enhanced Imaging and the Centre for Nanoscience and Quantum Information (NSQI).

Disclosures

The authors declare no conflicts of interest.

References

1. A. Rogalski, "Infrared detectors: status and trends," Prog. Quantum Electron. **27**(2-3), 59–210 (2003).
2. J. B. McManus, M. S. Zahniser, and D. D. Nelson, "Dual quantum cascade laser trace gas instrument with astigmatic Herriott cell at high pass number," Appl. Opt. **50**(4), A74–A85 (2011).
3. I. Ventrillard, P. Gorrotxategi-Carbajo, and D. Romanini, "Part per trillion nitric oxide measurement by optical feedback cavity-enhanced absorption spectroscopy in the mid-infrared," Appl. Phys. B **123**(6), 180 (2017).
4. M. M. J. W. van Herpen, S. Li, S. E. Bisson, and F. J. M. Harren, "Photoacoustic trace gas detection of ethane using a continuously tunable, continuous-wave optical parametric oscillator based on periodically poled lithium niobate," Appl. Phys. Lett. **81**(7), 1157–1159 (2002).
5. R. Furstenberg, C. Kendziora, M. Papantonakis, S. V. Stepnowski, J. Stepnowski, V. Nguyen, M. Rake, and R. A. McGill, "Stand-off Detection of Trace Explosives by Infrared Photo-thermal Spectroscopy," in Proceedings of IEEE Conference on Technologies for Homeland Security (IEEE, 465–471 (2009).
6. D. Fournier, A. C. Boccara, N. M. Amer, and R. Gerlach, "Sensitive in situ trace-gas detection by photothermal deflection spectroscopy," Appl. Phys. Lett. **37**(6), 519–521 (1980).
7. K. H. Fung and H.-B. Lin, "Trace gas detection by laser intracavity photothermal spectroscopy," Appl. Opt. **25**(5), 749–752 (1986).
8. F. G. Gebhardt and D. C. Smith, "Kinetic Cooling of a Gas by Absorption of CO_2 Laser Radiation," Appl. Phys. Lett. **20**(3), 129–132 (1972).
9. C. C. Davis, "Trace detection in gases using phase fluctuation optical heterodyne spectroscopy," Appl. Phys. Lett. **36**(7), 515–518 (1980).
10. C. C. Davis and S. J. Petuchowski, "Phase fluctuation optical heterodyne spectroscopy of gases," Appl. Opt. **20**(14), 2539–2554 (1981).
11. M. H. Dunn and M. Ebrahimzadeh, "Parametric Generation of Tunable Light from Continuous-Wave to Femtosecond Pulses," Science **286**(5444), 1513–1517 (1999).
12. D. D. Arslanov, M. Spunei, A. K. Y. Ngai, S. M. Cristescu, I. D. Lindsay, S. T. Persijn, K. J. Boller, and F. J. M. Harren, "Rapid and sensitive trace gas detection with continuous wave Optical Parametric Oscillator-based Wavelength Modulation Spectroscopy," Appl. Phys. B **103**(1), 223–228 (2011).
13. A. K. Y. Ngai, S. T. Persijn, G. von Basum, and F. J. M. Harren, "Automatically tunable continuous-wave optical parametric oscillator for high-resolution spectroscopy and sensitive trace-gas detection," Appl. Phys. B **85**(2-3), 173–180 (2006).
14. J. Peltola, M. Vainio, T. Hieta, J. Uotila, S. Sinisalo, M. Metsälä, M. Siltanen, and L. Halonen, "High sensitivity trace gas detection by cantilever enhanced photoacoustic spectroscopy using a mid-infrared continuous-wave optical parametric oscillator," Opt. Express **21**(8), 10240–10250 (2013).
15. D. J. M. Stothard, M. H. Dunn, and C. F. Rae, "Hyperspectral imaging of gases with a continuous-wave pump-enhanced optical parametric oscillator," Opt. Express **12**(5), 947–955 (2004).
16. G. von Basum, D. Halmer, P. Hering, M. Mürtz, S. Schiller, F. Müller, A. Popp, and F. Kühnemann, "Parts per trillion sensitivity for ethane in air with optical parametric oscillator cavity leak-out spectrometer," Opt. Lett. **29**(8), 797–799 (2004).
17. G. Robertson, M. J. Padgett, and M. H. Dunn, "Continuous-wave single resonant pump-enhanced type II LiB_3O_5 optical parametric oscillator," Opt. Lett. **19**(21), 1735–1737 (1994).
18. K. Schneider, P. Kramper, S. Schiller, and J. Mlynek, "Toward an optical synthesizer: a single-frequency parametric oscillator using periodically poled $LiNbO_3$," Opt. Lett. **22**(17), 1293–1295 (1997).
19. D. J. M. Stothard, I. D. Lindsay, and M. H. Dunn, "Continuous-wave pump-enhanced optical parametric oscillator with ring resonator for wide and continuous tuning of single-frequency radiation," Opt. Express **12**(3), 502–511 (2004).
20. F. Müller, G. von Basum, A. Popp, D. Halmer, P. Hering, M. Mürtz, F. Kühnemann, and S. Schiller, "Long-term frequency stability and linewidth properties of continuous-wave pump-resonant optical parametric oscillators," Appl. Phys. B: Lasers Opt. **80**(3), 307–313 (2005).
21. B. Edlén, "The Refractive Index of Air," Metrologia **2**(2), 71–80 (1966).
22. Light Machinery Inc, "Light Machinery Excellence in Lasers and Optics," https://lightmachinery.com/.

Optics EXPRESS

23. J. W. Thomas, A. Polak, G. M. Bonner, S. Enderle, M. H. Dunn, and D. J. M. Stothard, "Optical parametric oscillator-based trace detection of gases in the mid-infrared region using phase-fluctuation optical heterodyne spectroscopy," Proc. SPIE **10629**, 30 (2018).
24. J. W. Thomas, A. Polak, and D. J. M. Stothard, "Quantum cascade laser-based trace detection of gases in the deep-infrared region using phase fluctuation optical heterodyne spectroscopy," Proc. SPIE **11010**, 40 (2019).
25. H. Vahlbruch, *Squeezed Light for Gravitational Wave Astronomy* (Gottfried Wilhelm Leibniz Universität, 2008), Chap. 3.